Anal Bioanal Chem (2013) 405:4811–4822
DOI 10.1007/s00216-013-6842-0

RESEARCH PAPER

Discovery of safety biomarkers for realgar in rat urine using UFLC-IT-TOF/MS and ^{1}H NMR based metabolomics

Yin Huang · Yuan Tian · Geng Li · Yuanyuan Li · Xinjuan Yin · Can Peng · Fengguo Xu · Zunjian Zhang

Received: 30 December 2012 / Revised: 10 February 2013 / Accepted: 12 February 2013 / Published online: 13 March 2013
© Springer-Verlag Berlin Heidelberg 2013

Abstract As an arsenical, realgar (As_4S_4) is known as a poison and paradoxically as a therapeutic agent. However, a complete understanding of the precise biochemical alterations accompanying the toxicity and therapy effects of realgar is lacking. Using a combined ultrafast liquid chromatography (UFLC) coupled with ion trap time-of-flight mass spectrometry (IT-TOF/MS) and ^{1}H NMR spectroscopy based metabolomics approach, we were able to delineate significantly altered metabolites in the urine samples of realgar-treated rats. The platform stability of the liquid chromatography LC/MS and NMR techniques was systematically investigated, and the data processing method was carefully optimized. Our results indicate significant perturbations in amino acid metabolism, citric acid cycle, choline metabolism, and porphyrin metabolism. Thirty-six metabolites were proposed as potential safety biomarkers related to disturbances caused by realgar, and glycine and serine are expected to serve as the central contacts in the metabolic pathways related to realgar-induced disturbance. The LC/MS and NMR based metabolomics approach established provided a systematic and holistic view of the biochemical effects of realgar on rats, and might be employed to investigate other drugs or xenobiotics in the future.

Keywords Realgar · Metabolomics · Liquid chromatography–mass spectrometry · NMR · Urine · Biomarker

Introduction

The treatment of malignant diseases, e.g., cancer, generally involves the use of highly toxic drugs. Arsenic, for example, shows great toxic effects, especially with chronic exposure from industrial or natural sources, but exhibits striking therapeutic value in the treatment of hematopoietic malignancies. Realgar, an ore crystal containing more than 90 % tetraarsenic tetrasulfide (As_4S_4), is widely used alone or in combination with other herbal medicines as an oral remedy for cancer chemotherapy in traditional Chinese medicines and in Indian Ayurvedic medicines [1]. For long-term use of a drug in cancer therapy, the route and duration of administration are important factors that could influence patient compliance. According to the results of recent clinical trials [2, 3], realgar was found to be as effective as arsenic trioxide, which was approved by FDA for the treatment of relapsed or refractory acute promyelocytic leukemia, but with relatively better oral safety profiles even with long-term administration. These

Electronic supplementary material The online version of this article (doi:10.1007/s00216-013-6842-0) contains supplementary material, which is available to authorized users.

Y. Huang · Y. Tian · G. Li · Y. Li · X. Yin · C. Peng · F. Xu · Z. Zhang
Key Laboratory of Drug Quality Control and Pharmacovigilance, China Pharmaceutical University, Ministry of Education, Nanjing 210009, China

Y. Huang · Y. Tian · G. Li · Y. Li · X. Yin · C. Peng · F. Xu (✉) · Z. Zhang (✉)
Department of Pharmaceutical Analysis, China Pharmaceutical University, Tongjiaxiang No. 24, Nanjing 210009, China
e-mail: fengguoxu@gmail.com
e-mail: zunjianzhangcpu@hotmail.com

might give realgar an advantage over arsenic trioxide in maintenance treatment. However, in most systems of traditional medicine, poisonous substances are used with extreme caution because of issues with assessing potency and the measurement of a safe dose. In recent years, some cases of realgar poisoning caused by overdose, long-term use, and improper processing have been reported [4–6].

Some studies suggested that realgar exposure resulted in various arsenical metabolites in the urine [7]. It was believed that the metabolism of arsenic plays an important role in the toxicity of realgar, an arsenic-based drug. Much research focused on determining the blood or urinary arsenic levels as biomarkers of realgar exposure [8–10]. However, the metabolism of realgar in mammals is still unclear. The chemical forms of arsenicals determine their tissue accumulation and toxicity potentials, and thus the use of the total content of arsenic to evaluate the safety of realgar or realgar-containing medicines is inappropriate [11]. In such a case, it would be more meaningful to pay attention to the systemic metabolic response to realgar in a whole living biosystem.

Metabolomics is primarily concerned with identification and quantitation of small-molecule metabolites (smaller than 1,500 Da) in a biological specimen [12]. It facilitates the survey, explanation, and understanding of the global changes in plasma, tissue, and urinary metabotypes of biological systems in response to disease, pharmacological treatment, or toxicological insult. As a result, metabolomics has shown great potential applications in biomarker discovery for the diagnosis of a number of diseases, the elucidation of the clinicopatho genesis of diseases, and the assessment of exposure of biological systems to xenobiotics [13–16]. In our previous work, seven organic acids in rat urine were simultaneously quantified as biomarkers of realgar exposure [17]. Huo et al. [18] observed the alteration of amino acid neurotransmitters in brain tissues of immature rats treated with realgar. Recently, a metabolic profiling study using ^{1}H NMR spectroscopy by Wei et al. [19] reported a number of complex disturbances in the endogenous metabolites after an extremely high dose of realgar had been given for 7 days. Since a high dose of any compound could make it a poison, the major drawback of the study of Wei et al. was that the efficacy of a therapeutic dose of realgar under was not considered. Moreover, they failed to find an integrated metabolic pathway based on the altered metabolites. This might be because the NMR technique was relatively insensitive and some subtle variations of trace constituents were not evidenced with it [20].

In the current study, in order to have broad metabolic coverage and subsequently investigate the correlations of marker metabolites, liquid chromatography (LC)/mass spectrometry (MS) and NMR based metabolomics techniques were used to analyze urine samples collected from control rats and rats treated with different doses of realgar. The platform variability of both techniques was systematically investigated, and the data processing method was carefully optimized. Safety biomarkers were screened by statistical analysis, and the changes of their urinary levels were assessed in terms of the metabolic pathways being perturbed by realgar treatment.

Materials and methods

Chemicals and reagents

Realgar was obtained from Jiangsu Province Administration of Medicine, and had an As_4S_4 content of more than 90 %. 9-Fluorenylmethyloxycarbonyl-glycine, used as the internal standard for LC/MS analysis, and all the authentic standards were purchased from Sigma-Aldrich (St. Louis, MO, USA). NMR solvents, sodium salt of 3-trimethylsilylpropionic acid, and deuterium oxide, were also obtained from Sigma-Aldrich (St. Louis, MO, USA). Acetonitrile and methanol of high-performance LC grade were purchased from Merck (Darmstadt, Germany). Analytical grade formic acid, sodium dihydrogen phosphate, and disodium hydrogen phosphate were obtained from Nanjing Chemical Reagent. (Nanjing, China). Sodium carboxymethylcellulose (CMC-Na) and sodium azide were obtained from the Sinopharm Chemical Reagent (Shanghai, China). Deionized water was purified using a Milli-Q system (Millipore, Bedford, MA, USA).

Animal handling and sample collection

Animal care was performed in accordance with the Guide for the Care and Use of Laboratory Animals and was authorized by the Animal Ethics Committee of China Pharmaceutical University. Forty male Sprague-Dawley rats (weighing 220±20 g) were purchased from the experimental animal center of Qinglong Mountain (Nanjing, China) and housed in a room with an ambient temperature of 22±2 °C, 12 h light (7:00 to 19:00) and dark (19:00 to 7:00) cycles, and relative humidity of 50±5 %. Rats were acclimatized for 7 days in plastic cages and fed ad libitum with a standard rodent diet. Then they were randomly divided into four groups with ten rats in each group, and 20, 100, and 500 mgkg^{-1} bodyweight realgar suspended in 0.5 % (w/v) CMC-Na and CMC-Na only, respectively, were administered intragastrically once a day for 21 consecutive days

Urine samples were collected in ice-cooled vessels containing 1 % sodium azide on day 14 and stored at −80 °C prior to metabolomic analysis. All rats were euthanized after the urine samples had been collected. Blood from the euthanized rats was allowed to clot at 4 °C for 60 min and was then centrifuged (3,500g, 10 min at 4 °C) to remove any precipitates. The resultant serum samples were frozen at −80 °C until clinical chemistry analysis. The brain, heart, liver, and kidney were removed and used for

histological examination. Furthermore, samples were randomized for all treatment and analytical steps.

Analytical procedure for ultrafast LC–ion trap time-of-flight MS analysis

Sample preparation

Urine samples were thawed at room temperature and then centrifuged at 14,000*g* (Eppendorf 5430R, Germany) for 10 min at 4 °C. A 200-μL aliquot of supernatant was mixed with 50 μL of internal standard (20 μg/mL) and 550 μL of methanol. After vortexing, the solution was filtered through 0.22-μm nylon filter film, and then analyzed by LC/MS.

Apparatus and analytical conditions

A 7-μL aliquot of filtered urine was injected into a Shim-pack XR-ODS column (150 mm × 2.0 mm × 2.2 μm, Shimadzu, Japan) using a Shimadzu ultrafast LC–ion trap time-of flight MS system. The column and sample glass vials were maintained at 35 °C and 4 °C, respectively. The gradient duration was 30 min at a flow rate of 0.4 mL min^{-1} with the mobile phase containing water with 0.1 % formic acid (mobile phase A) and acetonitrile with 0.1 % formic acid (mobile phase B). From 0 to 1 min, mobile phase B was kept at 2 % and was then increased linearly to 40 % in the next 2 min. Then, mobile phase B was linearly increased to 98 % within 15 min and kept at 98 % for 5 min. At 23.1 min, the proportion of mobile phase B was adjusted to 2 % for equilibration for 7 min. Positive ionization mode and negative ionization mode mass spectra were obtained simultaneously in a full-scan operation with a scan range of 80–800 *m/z* by switching the interface voltage between 4.5 and −3.5 kV in each 0.1 s. The flow rate of the nebulizing gas (N_2) was 1.5 L min^{-1}. The temperatures of the curved desorption line and the heat block were both 200 °C, and the microchannel plate detector voltage was set to 1.70 kV. The pressure of the drying gas (N_2) was 150 kPa, and the ion accumulation time was set to 30 ms. Ultra-high-purity argon was employed as both the ion cooling gas and the collision gas. Mass spectra and chromatograms were acquired and processed with LCMSsolution version 3.0 (Shimadzu, Japan).

Data preprocessing and analysis

The raw LC/MS data were processed by Profiling Solution version 1.1 (Shimadzu, Japan) for peak deconvolution and alignment. The primary parameters were as follows: width (5 s), slope (2,000 min^{-1}), ion *m/z* tolerance (20 mDa), ion retention time tolerance (0.3 min), and ion intensity threshold (10,000 counts). Other parameters were set as the default. A matrix consisting of matched ion features with retention time, *m/z* value, and corresponding intensities was generated and exported to an Excel table. These data were handled according to the "80 % rule": only the variables with values above zero in at least 80 % of each group were kept for the following analysis. Then, the individual ion fragment intensity was normalized to the intensity of the internal standard in the relative chromatogram. After normalization, variables with relative standard deviation (RSD) higher than 30 % in quality control (QC) samples were removed. Before mean-centering the variables, we performed log transformation (with an offset of 20) to stabilize the variance throughout the intensity range.

The two preprocessed data sets—positive electrospray ionization (ESI+) and negative electrospray ionization (ESI-) modes—were used as an input for SIMCA-P version 13.0 (Umetrics, Sweden) to perform principal components analysis (PCA) and orthogonal partial least squares discriminant analysis (OPLS-DA). Two-dimensional scores plots were used to visualize the relative importance of the different sources of variation. The corresponding variable importance in the projection (VIP value) was calculated in the OPLS-DA model. Further, the nonparametric Kruskal–Wallis rank sum test was performed to determine the significance of each metabolite, and the relevant false discovery rates based on the *p* value were estimated in the context of multiple testing. A potential metabolic biomarker was selected when the value of its VIP was more than 1.00 and the false discovery rate was less than 0.05.

Identification of potential biomarkers

Identification of the marker metabolites was achieved through a mass-based search followed by manual verification. First, the *m/z* value of the molecular ion of interest was searched against four databases: the Human Metabolome Database (HMDB), METLIN, the Madison Metabolomics Consortium Database (MMCD), and LIPID MAPS. Then, the putative identifications were verified by comparing the MS^n fragmentation patterns and retention time with those of authentic standard compounds. The heat map representation was used to visualize the variation in the levels of important metabolites in control and realgar-treated groups.

Analytical procedure for ^{1}H NMR analysis

Sample preparation

Frozen urine samples were thawed at room temperature and 550 μL of urine was buffered with 150 μL of a 1 M phosphate buffer in deuterium oxide (pH 7.0) containing 10 mM 3-trimethylsilylpropionic acid as a shift-lock reagent. Any particulate matter was removed by centrifugation (14,000*g*, 10 min at 4 °C) and 500 μL of the supernatant was transferred into a 5-mm NMR tube.

Apparatus and analytical conditions

NMR spectra were acquired with a Bruker Avance 500 spectrometer operating at 500.13 MHz for ^{1}H observation, at 298 K. For each sample, a standard 1D ^{1}H NMR spectrum was acquired, using a water suppression pulse sequence with water irradiation during the relaxation delay and mixing time (noesypr1d in the Bruker library, spectral width (SWH) 5,482.5 Hz, time domain (TD) 32,738 data points, relaxation delay 4 s, mixing time 100 ms, 80 scans). Instrument control, data recording, and phase and baseline correction were done with TopSpin version 2.1 (Bruker, Germany).

Data preprocessing and analysis

To build the data matrix, spectra were segmented into regions of 0.01 ppm using MestreNova version 8.0 (Mestrelab Research, Spain) and buckets were generated in the regions from 9.5 to 6.5 ppm and from 4.5 to 0.5 ppm, respectively, to exclude the water artifact and the broad urea signal. Some of these buckets were merged to larger buckets in regions where chemical shift drifts (due to small pH differences or variations in sample ionic strength) were observed. Then, each variable was normalized to the total area in order to allow a spectrum-to-spectrum comparison. After the data has been scaled to unit variance, both univariate and multivariate statistical analysis were applied to the data set and were performed in the same manner as described for the LC/MS data.

Identification of potential biomarkers

The data acquired using NMR spectroscopy are highly reproducible in both intralaboratory and interlaboratory experiments, with less than 2 % variation between laboratories even when spectrometers with different field strengths are used [21, 22]. References of pure compounds from the metabolic profiling AMIX spectral database (Bruker), HMDB, and the Chenomx database were used for metabolite identification.

Method validation

QC samples were prepared by combining equal aliquots from all urine samples in the study and were analyzed before, during, and after the run. Data obtained from the QC samples were used to assess the stability of the LC/MS and NMR platform over the run through examination of chromatograms and spectra as well as univariate and multivariate analysis.

Furthermore, for LC/MS analysis, after finding potential biomarkers as described in Table 1, we selected several metabolites among them which had good intensity and peak shape in the chromatogram to check the recovery and reproducibility during membrane filtration. The metabolites selected were as follows: citric acid, hippuric acid, α-ketoglutaric acid, taurine, and coproporphyrin.

Clinical chemistry and histopathology

Biochemical indices of serum samples were analyzed with a Hitachi 7100 automatic analyzer (Tokyo, Japan) including alanine aminotransferase (ALT), aspartate aminotransferase (AST), alkaline phosphatase (ALP), blood urea nitrogen, creatinine, uric acid, total protein, albumin, triglyceride, and total cholesterol. Dunnett's test was conducted to compare clinical chemical data between dosed groups and the control group.

The brain, heart, liver, and kidney slices of control and realgar-treated rats were fixed in 10 % formalin, stained with hematoxylin–eosin, and examined by light microscopy for histopathology assessment.

Results and discussion

Ultrafast LC–ion trap time-of flight MS analysis

The inspection of the chromatographs of QC samples with regard to retention times, intensities, and peak shapes indicated good overall analytical platform stability. The optimized gradient allowed separation for a high number of peaks (see Electronic Supplementary Material, Fig. S1).

Data preprocessing

After peaks had been picked with Profiling Solution and screened with the "80 % rule" and "RSD≤30 %", 379 (ESI+) and 383 (ESI-) metabolite variables (*m*/*z*–retention time pairs) were obtained for the urine samples. Multivariate statistical analysis was used to extract meaningful information from these large data sets. To produce adequate models of the data, the measurement errors should have a uniform variance across the data set (homoscedastic noise). However, the concentration of metabolites can range over many orders of magnitude, and higher-concentration metabolites may have higher variation, causing the variables with large intensities to have the greatest influence on the results of PCA or OPLS-DA. Therefore, it is important to scale the variable intensities before analysis to avoid selection of the most abundant metabolites as significant. Three methods were attempted in this study: mean-centering, Pareto scaling, and mean-centering after log transformation [23]. In Fig. 1a, the most intense variables (on the right) exhibit high standard deviation compared with the rest of the data set. To reduce the importance of them, Pareto scaling was used, where each variable was divided by the square root of the standard deviation. However, this did not change the overall

Table 1 Potential biomarkers detected by ultrafast liquid chromatography–ion trap time-of flight mass spectrometry analysis

Metabolite	Related pathway	Ion (*m*/*z*)	Retention time (min)	ESI mode
1-Methyladenosine	Adenine metabolism	282.1243	1.22	+
3-Methyluridine	RNA biosynthesis	259.1075	8.92	+
Coproporphyrin	Porphyrin metabolism	655.2786	17.62	+
Creatine	Glycine and serine metabolism	132.0997	1.58	+
Hippuric acid	Phenylalanine metabolism	180.0630	9.64	+
Inosine	Purine metabolism	269.1280	9.88	+
Kynurenic acid	Tryptophan metabolism	190.0458	9.82	+
Methionine	Methionine metabolism	150.0616	1.43	+
N-Acetyl-L-methionine	Methionine metabolism	192.0999	8.72	+
Trigonelline	Niacin metabolism	138.0552	1.19	+
Tryptophan	Tryptophan metabolism	205.0923	8.44	+
Anserine	Alanine metabolism	239.1281	19.85	−
Citric acid	Citric acid cycle	191.0205	1.13	−
Decenedioic acid	Fatty acid oxidation	199.0985	11.62	−
D-Glucuronic acid 1-phosphate	Glucuronidation	273.0064	11.93	−
Gluconic acid	Glucose oxidation	195.0518	1.04	−
Lactic acid dimer	Pyruvate metabolism	179.0573	1.01	−
Mannitol	Fatty alcohol metabolism	217.0454	0.95	−
N^4-Acetylcytidine	Transfer RNA degradation	284.0577	11.21	−
Pantothenic acid	Pantothenate and coenzyme A biosynthesis	218.1035	8.31	−
Phenyl glucuronide	Glucuronidation	269.0655	9.36	−
Taurine	Bile acid biosynthesis	124.0112	0.94	−
Xanthurenic acid	Tryptophan metabolism	204.0307	9.42	−
α-Ketoglutaric acid	Citric acid cycle	145.0179	1.67	−

ESI electrospray ionization

appearance of the plot (Fig. 1b), with high-intensity features still exhibiting high standard deviation, although the range of variation was smaller. Figure 1c shows the plot after log-transforming the data with an offset of 20 (this value was chosen to avoid an increase in the standard deviation for low-intensity signals) and mean-centering the variables. After this transformation, standard deviations were uniform across the range of intensities and the focus would not be on high-intensity signals. Similar effects were observed for the ESI- data set, and log transformation was also used for it.

Statistical analysis

As a first step in chemometric analysis, PCA, an unsupervised multivariate data analysis technique, was performed to visualize grouping trends and outliers in data. Principal component 1 versus principal component 2 scores plots of the urine samples are shown in Fig. 2a and b. The QC samples clustered tightly in both modes, illustrating the stability of the LC/MS platform throughout the whole run. For ESI+ mode, the first two principal components separated the control and realgar-treated groups well, whereas the difference between them is not rigid in the scores plot for ESI- mode. This might because PCA did not use the class information regarding the data. As such, OPLS-DA, a supervised analysis technique, was employed to divide the different groups of urine samples and aid the screening of potential marker metabolites.

Figure 2d and e displays the results of the OPLS-DA, showing an appreciable separation of the data pertaining to the four groups. The model statistics, R^2X, R^2Y, and Q^2, indicate that the models are robust and not the result of statistical overfitting. In both OPLS-DA models, the control and high-dose groups are located on the outer edges of the plots, whereas the low-dose and mid-dose groups are situated near the center, suggesting that the metabolic profiles changed in a dose-dependent manner as a result of the administration of realgar. After screening with "VIP>1.00" and "$p<0.05$," we obtained 157 (ESI+) and 177 (ESI-) metabolite variables for further identification.

Potential biomarkers

Twenty-four potential biomarkers are summarized in Table 1 with their corresponding retention time, *m*/*z*,

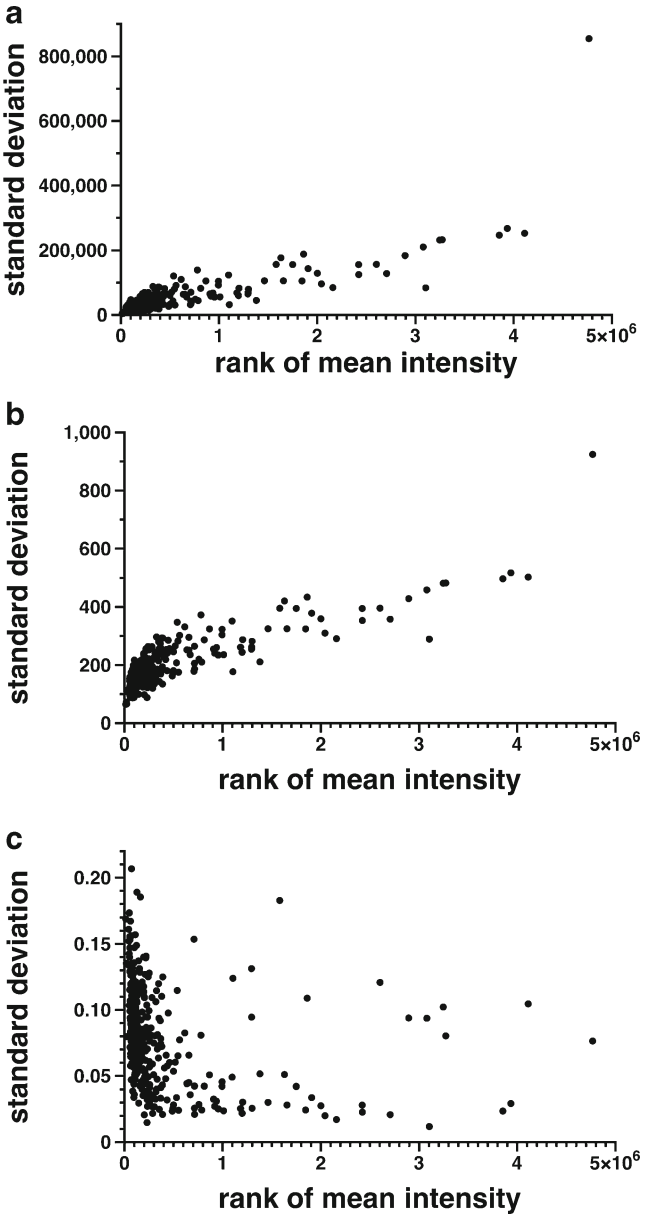

Fig. 1 Standard deviations versus rank of mean intensities for the replicate injections of the quality control sample for the organic extracts analyzed in positive electrospray ionization (ESI+) mode. Each *dot* represents one variable. Standard deviations were calculated on **a** mean-centered data, **b** Pareto-scaled data, and **c** mean-centered data after log transformation with an offset of 20

ionization mode, and related metabolic pathways. Fifteen of the 24 marker metabolites were identified by authentic standards, and the others were deduced on the basis of accurate molecular weights, MS/MS fragments, and metabolomics databases. Part A of Fig. 3 illustrates in a heat map the changes in the concentrations of these potential biomarkers in different groups. Reduced urinary excretion patterns of several metabolites, from kynurenic acid to pantothenic acid, were detected in rats treated with realgar, whereas the levels of the other metabolites were significantly increased.

Most of the marker metabolites were organic acids that play important roles in various biochemical processes. For example, tryptophan is an essential amino acid for many organisms (including humans). It not only acts as a building block in protein biosynthesis, but also functions as a biochemical precursor for some compounds, such as serotonin, niacin, and auxin [24]. Kynurenic acid and xanthurenic acid are connected within the tryptophan catabolic pathway. Downregulation of both kynurenic acid and tryptophan combined with the upregulation of xanthurenic acid indicated that the tryptophan metabolism was disturbed by the administration of realgar. Creatine is an amino acid that is synthesized mainly in the liver. As the level of urinary creatine has been shown to increase in multiple hepatic toxicity studies [25–27], the elevated creatine levels observed in dosed rats might reflect the hepatotoxicity of realgar. Besides organic acids, some other kinds of compounds were also found to be potential biomarkers. Increased levels of coproporphyrin, a porphyrin metabolite, indicated abnormalities of porphyrin metabolism. A published study showed that the effect of arsenic on heme biosynthesis resulting in increased urinary excretion of porphyrin [28].

Method validation

The retention time of metabolites was checked by injection of the standard solution for citric acid, hippuric acid, α-ketoglutaric acid, taurine, and coproporphyrin. Recovery and reproducibility of analytes by filtration were systematically studied, and the results are presented in Table 2. Recovery of analytes was found to be more than 85 %, with reproducibility (RSD) less than 15 %.

^{1}H NMR analysis

A number of biomolecules were observed in the ^{1}H NMR spectra of urine samples (see Electronic Supplementary Material, Fig. S2). After the binning, the spectrum dimension was reduced to 698, with the 0.01-ppm value of each bin being considered as the variable. To evaluate the differences in the acquired spectra, data were initially analyzed using PCA. As shown in Fig. 2c, the QC samples cluster almost together near the center of the plot, indicating the high stability of the NMR platform. Two outliers, which might be due to the individual variation after administration of high-dose realgar, were easily distinguished, whereas the four groups overlapped with each other and were not apparently separated. Thus, OPLS-DA was subsequently conducted using the dataset without the outliers. The scores plot (Fig. 2f) showed that the distributions of urine samples were dose-related, which was similar to what was observed in LC/MS analysis. Then, the data set was screened with a

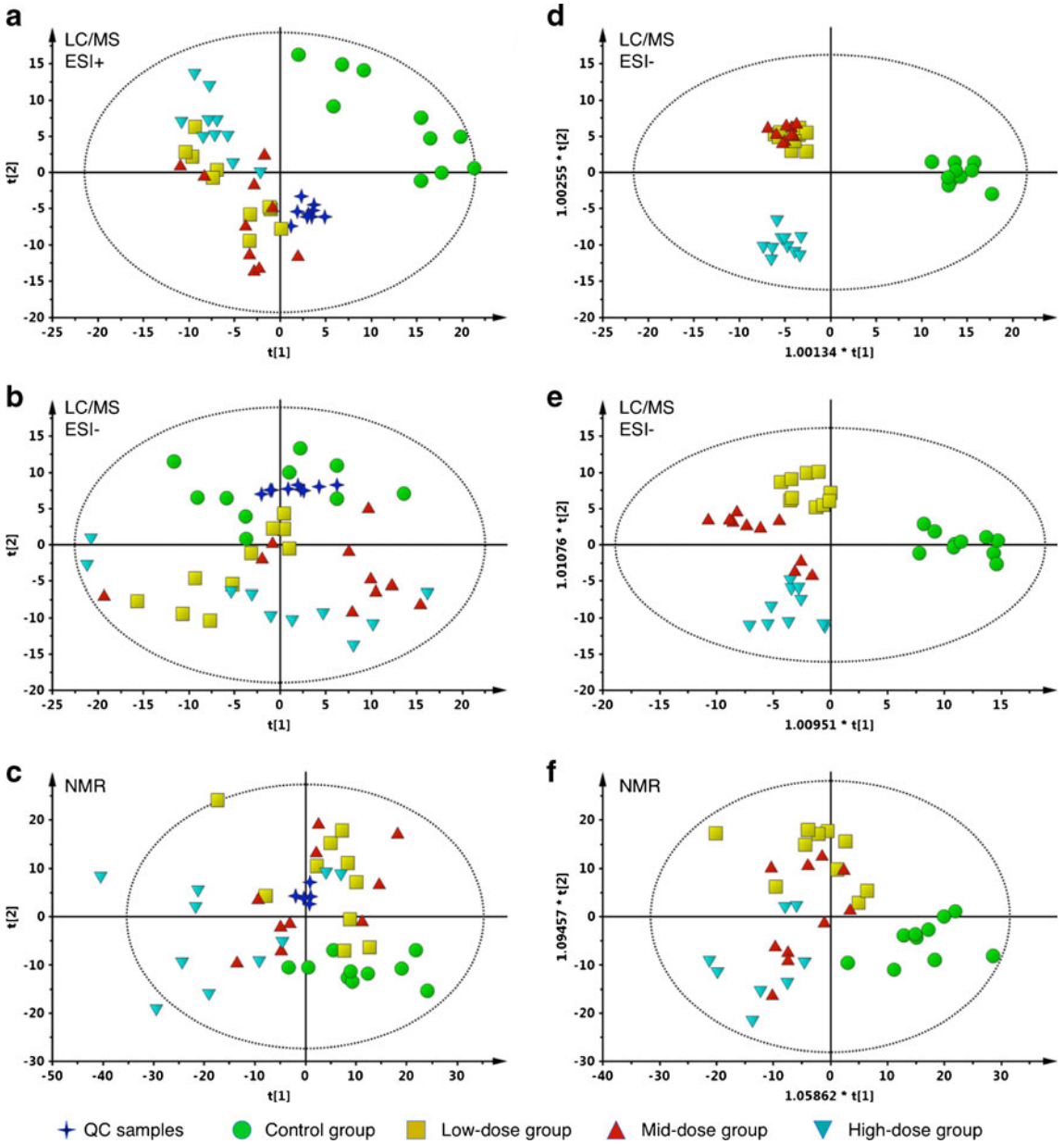

Fig. 2 Scores plots of principal components analysis (**a**–**c**) and orthogonal partial least squares discriminant analysis (**d**–**f**) models with the statistical parameters as follows: **a** R^2X=0.633, Q^2=0.492; **b** R^2X=0.659, Q^2=0.456; **c** R^2X=0.704, Q^2=0.513; **d** R^2X=0.594, R^2Y=0.596, Q^2=0.824; **e** R^2X=0.59, R^2Y=0.822, Q^2=0.76; f R^2X=0.487, R^2Y=0.592, Q^2=0.399. *ESI-* negative electrospray ionization, *LC/MS* liquid chromatography/mass spectrometry, *QC* quality control

VIP value larger than 1.0 and a p value less than 0.05, leaving 179 metabolite variables for further identification.

With spectral databases of authentic substances, 18 potential biomarkers were identified from the NMR spectra (Table 3). The intensities of them in different groups of urine samples are shown in part B of Fig. 3. From alanine to pyruvic acid, the concentrations of these metabolites decreased with increasing dose of realgar, whereas the other potential biomarkers exhibited the opposite tendency. Of all these potential biomarkers, 12 metabolites were detected only by the NMR technique, most of which are polar compounds with low molecular weight. For instance, acetate is a derivative of acetic acid, which is one of the simplest carboxylic acids. When acetyl coenzyme A (acetyl-CoA) derived from glycolysis and lipid β-oxidation exceeds the capacity of the citric acid cycle, it will be hydrolyzed to acetate by acetyl-CoA hydrolase. Acetone is one of the ketone bodies that are also produced by excess acetyl-CoA. The levels of acetate and acetone were significantly increased with a decrease in the level of formic acid that could be connected to acetyl-CoA by acetyl-CoA C-acetyltransferase, suggesting that the system was attempting

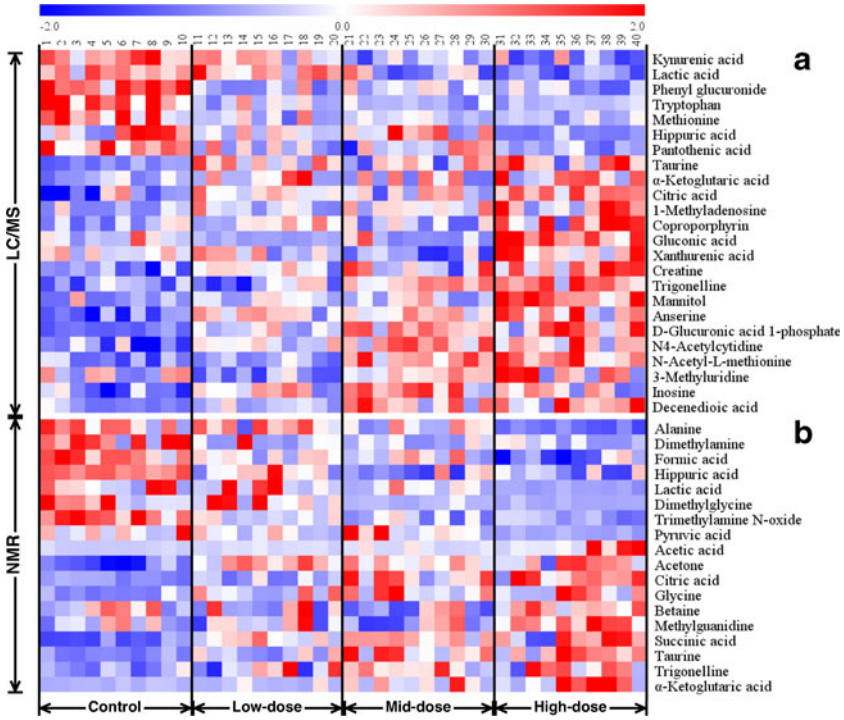

Fig. 3 The heat map shows altered concentrations of potential biomarkers detected by LC/MS (**a**) and NMR spectroscopy (**b**) in different groups of rats

to replenish acetyl-CoA levels after the treatment with realgar. Trimethylamine *N*-oxide (TMAO) is an oxidation product of trimethylamine, which is derived from choline by gut bacteria [29]. The precursors of hippuric acid are also produced by gut bacteria [30]. The decreased urinary excretions of TMAO and hippuric acid in dosed animals were considered due to realgar-induced disruption in the intestinal environment, because anti-inflammatory function is one of the commonest features for realgar [31].

Serum biochemical parameters and histopathological tests

Of all the serum biochemical parameters measured, the concentrations of ALT, AST, ALP, albumin, and uric acid were significantly increased after treatment with mid-dose and high-dose realgar (Table 4). ALT and AST are usually used to diagnose liver injury, and uric acid concentration corresponds closely to kidney damage. Elevated ALP and albumin levels indicate the blockage of bile ducts and the

Table 2 Recovery and reproducibility for the sample preparation step in ultrafast liquid chromatography–ion trap time-of flight mass spectrometry analysis (n=6)

Metabolites	Concentration (μg mL^{-1})	Recovery (%)	RSD (%)
Citric acid	2	89.1	9.2
	100	90.8	6.0
	200	91.5	6.5
Hippuric acid	0.5	88.7	13.2
	20	87.6	10.4
	50	90.0	5.5
α-Ketoglutaric acid	0.5	88.3	10.2
	20	85.1	7.4
	50	86.1	6.4
Taurine	2	89.5	7.5
	100	92.7	8.3
	200	93.0	5.1
Coproporphyrin	0.1	89.2	11.7
	4	88.2	6.7
	10	84.9	7.5

RSD relative standard deviation

Table 3 Potential biomarkers detected by ^{1}H NMR analysis

Metabolite	Related pathway	^{1}H chemical shift (ppm) and coupling
Acetate	Pyruvate metabolism	1.93 (s)
Acetone	Ketone body metabolism	2.23 (s)
Alanine	Alanine metabolism	1.49 (d), 3.79 (t)
Betaine	Betaine metabolism	3.28 (s), 3.91 (s)
Citric acid	Citric acid cycle	2.53 (d), 2.69 (d)
Dimethylamine	Choline metabolism	2.72 (s)
Dimethylglycine	Betaine metabolism	2.95 (s), 3.75 (s)
Formic acid	Folate metabolism	8.45 (s)
Glycine	Alanine metabolism	3.58 (s)
Hippuric acid	Phenylalanine metabolism	3.96 (d), 7.55 (m), 7.63 (t), 7.82 (m), 8.52 (s)
Lactic acid	Pyruvate metabolism	1.34 (d), 4.13 (d)
Methylguanidine	Protein catabolism	2.85 (s)
Pyruvic acid	Pyruvate metabolism	2.39 (s)
Succinic acid	Citric acid cycle	2.42 (s)
Taurine	Bile acid biosynthesis	3.25 (t), 3.41 (t)
Trigonelline	Niacin metabolism	4.43 (s), 8.07 (dd), 8.82 (m), 8.83 (m), 9.11 (s)
Trimethylamine *N*-oxide	Choline metabolism	3.27 (s)
α-Ketoglutaric acid	Citric acid cycle	2.46 (t), 3.02 (t)

s singlet, *d* doublet, *t* triplet, *q* quartet, *m* multiplet

perturbation of protein biosynthesis and catabolism, respectively. The serum biochemical results suggested that mild injuries to the liver and kidney could be caused by administration of realgar and they were aggravated with increasing dose, whereas the distinction between control and low-dose groups was not clear. For the histopathological tests, no significant evidence was observed. Therefore, the results from metabolomic analysis were more sensitive than histopathology and clinical chemistry tests.

Effects of realgar on the metabolic pathway

We generated a correlation matrix using Pearson's correlation analysis for the marker metabolites and biochemical parameters to create a compendium metabolic profile that integrates the complementary information from the LC/MS, NMR, and clinical chemistry analytical methods. The plot (Fig. 4) reveals a wide range of correlation coefficients among the metabolites and biochemical parameters, ranging from 1.0 (maximum positive correlation) to −1.0 (maximum anticorrelation), with 0 indicating no correlation. Subsequently, interpretation of the metabolic pathway of marker metabolites was performed on the basis of their correlations and the metabolomics database.

As shown in Fig. 5, a number of endogenous metabolites involved in various metabolic pathways can be affected by realgar exposure. Decreased levels of pyruvic acid, lactic acid, formic acid, and alanine were accompanied by elevated urinary

Table 4 Serum biochemical parameters in control and reaglar-treated rats

Parameters	Control	Reaglar-treated		
		Low dose	Mid dose	High dose
Alanine aminotransferase (IU L^{-1})	26.2±4.46	27.4±3.92	35.1±4.12*	48.5±10.81**
Aspartate aminotransferase (IU L^{-1})	115.1±18.26	132.4±22.52	130.5±13.32	165.9±11.66**
Alkaline phosphatase (IU L^{-1})	77.4±16.47	82.3±15.41	128.6±43.33*	194.3±64.80**
Blood urea nitrogen (mM)	5.95±0.81	5.72±0.55	5.721±0.64	6.61±0.80
Creatinine (μM)	74.7±3.68	78.9±5.04	79.1±3.87	77.8±5.59
Uric acid (μM)	111.8±14.12	107.4±10.27	187.2±81.37*	196.1±88.23*
Total protein (g L^{-1})	63.0±1.25	65.5±1.78	65.3±3.40	64.2±3.01
Albumin (g L^{-1})	32.3±1.25	32.2±1.39	34.9±0.88**	36.0±1.76**
Triglyceride (mM)	0.82±0.13	1.01±0.31	0.86±0.13	1.23±0.70
Total cholesterol (mM)	1.66±0.14	1.69±0.23	1.62±0.15	1.63±0.29

Data are presented as the mean ± the standard deviation of $n=10$ animals per group. Statistical analysis was performed by one-way analysis of variance followed by Dunnett's test

*$p<0.05$ for significant difference from the control group; **$p<0.01$ for significant difference from the control group

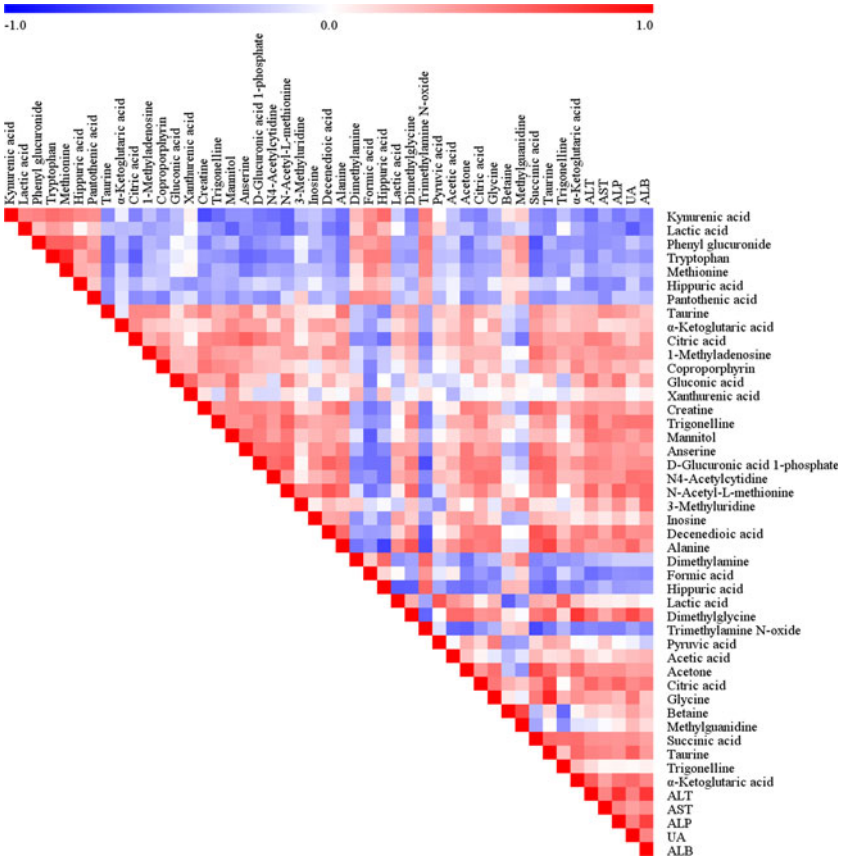

Fig. 4 Pearson's correlations of serum biochemical parameters and marker metabolites detected by LC/MS and NMR spectroscopy in rat urine. *ALB* albumin, *ALP* alkaline phosphatase, *ALT* alanine aminotransferase, *AST* aspartate aminotransferase, *UA* uric acid

excretion of citric acid cycle intermediates, including citric acid, succinic acid, and α-ketoglutaric acid. This indicated that the trend of pyruvate metabolism was towards the formation of acetyl-CoA, and consequently resulted in an expanded citric acid cycle pool. The abundant acetyl-CoA can be converted to acetate and ketone bodies, and therefore leads to an increase of

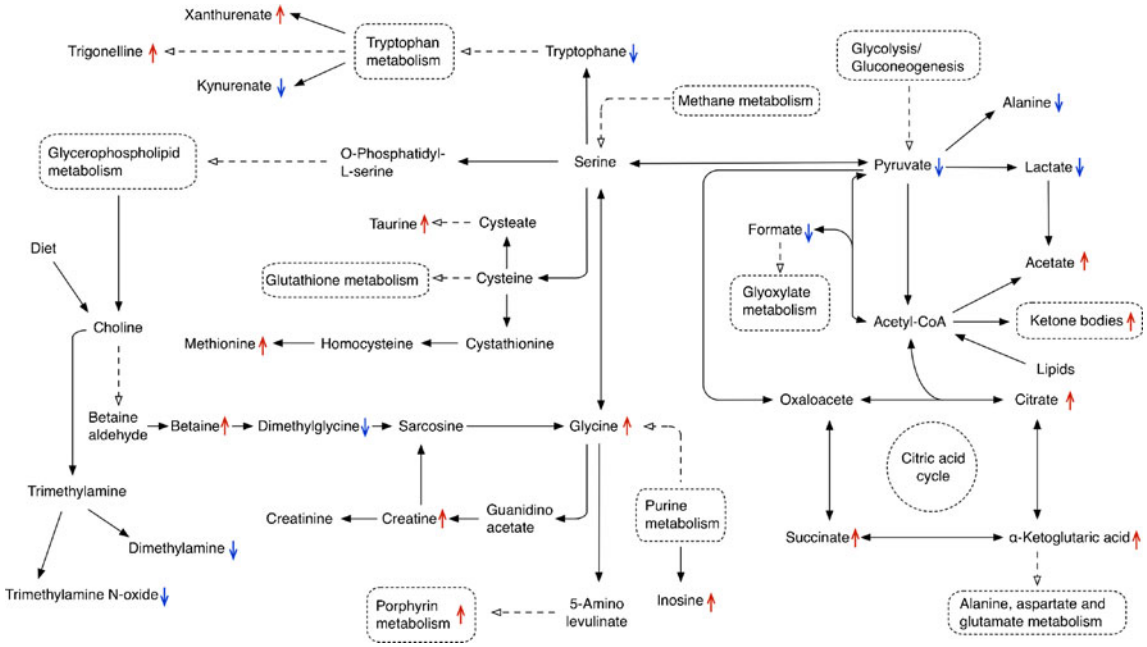

Fig. 5 The integrated metabolic pathway related to realgar-induced biochemical perturbation. Elevation (*up arrows*) and reduction (*down arrows*) of the levels of metabolites as observed in realgar-treated rats are indicated. *CoA* coenzyme A

their levels in urine. Choline is a basic constituent of lecithin, and plays an important role in the integrity of cell membranes and lipid metabolism [32]. A previous study reported that realgar exposure was able to lead to enhanced membrane permeability and altered membrane structure [33]. Although choline was not detected in rat urine, some important metabolites in choline metabolism were observed, such as betaine, dimethylglycine, and TMAO. The changes of these metabolites levels were reflected the disturbance to the choline metabolism, and this was likely related to realgar-induced membrane toxicity. All these results were in good agreement with reported works [9, 19, 34].

The new discovery of this study is that amino acids, especially glycine and serine, have a very important role in realgar-induced perturbation of biochemical pathways. Glycine is a nonessential amino acid involved in the body's production of DNA, phospholipids, and collagen, and in release of energy. Serine is a nonessential amino acid derived from glycine. Like all the amino acid building blocks of proteins and peptides, they can become essential under certain conditions, and are thus important in maintaining health and preventing disease. The findings of altered levels of serine and glycine in patients with psychiatric disorders and the severe neurological abnormalities in patients with defects of serine synthesis underscore the importance of serine in brain development and function [35, 36]. A recent study also reported that the neurotoxicity induced by realgar was associated with its effects on amino acid neurotransmitters [18]. From Fig. 4, it is obvious that almost all of the biochemical parameters and marker metabolites (except xanthurenic acid) have significant correlations with glycine, and Fig. 5 shows that glycine and serine serve as the central contacts for all metabolic pathways related to realgar-induced disturbance. In addition, coproporphyrin, which could be used as an early warning biomarker of chronic arsenic exposure in humans [28], seems to be a good biomarker for clinical patients taking realgar or realgar-containing medicines. The gradually increased levels of coproporphyrin from the control to the high-dose group (Fig. 4) also support it as a sensitive biomarker of realgar exposure. However, further investigations are needed to confirm whether coproporphyrin and other marker metabolites are competent biomarkers, because many urinary metabolites are sensitive to the effect of dietary intake or other physiological conditions such as age, gender, and demographic characteristics [37].

Conclusions

In this study, a urinary metabolomics approach, combined with serum biochemical and histopathological tests, was employed to investigate the metabolic disturbances after repeating oral administration of realgar. Significant dose-dependent changes were found in both LC/MS and NMR urine metabolite profiles. Thirty-six potential biomarkers were discovered, 24 of which were structurally identified by authentic standards or MS^n analysis. These metabolites demonstrated that abnormal metabolism occurred in various pathways, including the citric acid cycle, tryptophan metabolism, and porphyrin metabolism. Glycine and serine were proposed as key metabolites related to realgar-induced disturbance. Moreover, detection of systemic perturbation by metabolomics appeared to be more sensitive, i.e., detection was possible in the low-dose group, compared with clinical chemistry and histopathological assessments. The combination of LC/MS and NMR techniques on rat urine samples provides a powerful means of revealing changes in the metabolome due to realgar efficacy and toxicity.

Acknowledgment This work was supported by the Central University Foundation for Fundamental Research of China (no. JKY2009027).

References

1. Liu J, Lu Y, Wu Q, Goyer RA, Waalkes MP (2008) Mineral arsenicals in traditional medicines: orpiment, realgar, and arsenolite. J Pharmacol Exp Ther 326:363–368
2. Luo X-Q, Ke Z-Y, Huang L-B, Guan X-Q, Zhang Y-C, Zhang X-L (2009) Improved outcome for Chinese children with acute promyelocytic leukemia: a comparison of two protocols. Pediatr Blood Cancer 53:325–328
3. Hu J, Liu Y-F, Wu C-F et al (2009) Long-term efficacy and safety of all-trans retinoic acid/arsenic trioxide-based therapy in newly diagnosed acute promyelocytic leukemia. Proc Natl Acad Sci U S A 106:3342–3347
4. Zhang Y-N, Sun G-X, Huang Q, Williams PN, Zhu Y-G (2011) A cultural practice of drinking realgar wine leading to elevated urinary arsenic and its potential health risk. Environ Int 37:889–892
5. Lu Y, Shi J, Shi J, Liu J (2011) Safety evaluation of realgar-and cinnabar-containing traditional Chinese medicine. China J Chin Mater Med 36:3402–3405
6. Liang A, Li C, Wang J, Xue B, Li H, Yang B, Wang J, Xie Q, Nilsen OG (2011) Toxicity study of realgar. China J Chin Mater Med 36:1889–1894
7. Koch I, Sylvester S, Lai VWM, Owen A, Reimer KJ, Cullen WR (2007) Bioaccessibility and excretion of arsenic in Niu Huang Jie Du Pian pills. Toxicol Appl Pharmacol 222:357–364
8. Zhang J, Zhang X, Ni Y, Yang X, Li H (2007) Bioleaching of arsenic from medicinal realgar by pure and mixed cultures. Process Biochem 42:1265–1271
9. Liu J, Liang S-X, Lu Y-F, Miao J-W, Wu Q, Shi J-S (2011) Realgar and realgar-containing Liu-Shen-Wan are less acutely toxic than arsenite and arsenate. J Ethnopharmacol 134:26–31
10. Wu J-Z, Ho PC (2004) Speciation of inorganic and methylated arsenic compounds by capillary zone electrophoresis with indirect UV detection. J Chromatogr A 1026:261–270
11. Tse W-P, Cheng CHK, Che C-T, Lin Z-X (2008) Arsenic trioxide, arsenic pentoxide, and arsenic iodide inhibit human keratinocyte proliferation through the induction of apoptosis. J Pharmacol Exp Ther 326:388–394

12. Kaddurah-Daouk R, Kristal BS, Weinshilboum RM (2008) Metabolomics: a global biochemical approach to drug response and disease. Annu Rev Pharmacol Toxicol 48:653–683
13. Zgoda-Pols JR, Chowdhury S, Wirth M, Milburn MV, Alexander DC, Alton KB (2011) Metabolomics analysis reveals elevation of 3-indoxyl sulfate in plasma and brain during chemically-induced acute kidney injury in mice: investigation of nicotinic acid receptor agonists. Toxicol Appl Pharmacol 255:48–56
14. Wang X, Wang H, Zhang A, Lu X, Sun H, Dong H, Wang P (2012) Metabolomics study on the toxicity of aconite root and its processed products using ultraperformance liquid-chromatography/electrospray-ionization synapt high-definition mass spectrometry coupled with pattern recognition approach and ingenuity pathways analysis. J Proteome Res 11:1284–1301
15. Ressom HW, Xiao JF, Tuli L et al (2012) Utilization of metabolomics to identify serum biomarkers for hepatocellular carcinoma in patients with liver cirrhosis. Anal Chim Acta 743:90–100
16. Rupérez FJ, Ramos-Mozo P, Teul J et al (2012) Metabolomic study of plasma of patients with abdominal aortic aneurysm. Anal Bioanal Chem 403:1651–1660
17. Huang Y, Tian Y, Zhang Z, Peng C (2012) A HILIC-MS/MS method for the simultaneous determination of seven organic acids in rat urine as biomarkers of exposure to realgar. J Chromatogr B 905:37–42
18. Huo T, Chang B, Zhang Y, Chen Z, Li W, Jiang H (2012) Alteration of amino acid neurotransmitters in brain tissues of immature rats treated with realgar. J Pharm Biomed Anal 57:120–124
19. Wei L, Liao P, Wu H, Li X, Pei F, Li W, Wu Y (2009) Metabolic profiling studies on the toxicological effects of realgar in rats by (1)H NMR spectroscopy. Toxicol Appl Pharmacol 234:314–325
20. Powers R (2009) NMR metabolomics and drug discovery. Magn Reson Chem 47(Suppl 1):S2–S11
21. Keun HC, Ebbels TMD, Antti H et al (2013) Analytical reproducibility in 1H NMR-based metabonomic urinalysis. Chem Res Toxicol 15:1380–1386
22. Dumas M-E, Maibaum EC, Teague C et al (2006) Assessment of analytical reproducibility of 1H NMR spectroscopy based metabonomics for large-scale epidemiological research: the INTERMAP Study. Anal Chem 78:2199–2208
23. Masson P, Spagou K, Nicholson JK, Want EJ (2011) Technical and biological variation in UPLC-MS-based untargeted metabolic profiling of liver extracts: application in an experimental toxicity study on galactosamine. Anal Chem 83:1116–1123
24. Curzon G, Knott PJ (1974) Effects on plasma and brain tryptophan in the rat of drugs and hormones that influence the concentration of unesterified fatty acid in the plasma. Br J Pharmacol 50:197–204
25. Liu X, Xue X, Gong L, Qi X, WU Y, Xing G, Luan Y, Xiao Y, Wu X, LI Y 1H NMR-based metabolomic analysis of triptolide-induced toxicity in liver-specific cytochrome P450 reductase knockout mice. Metabolomics 1–12
26. Fukuda S, Nakanishi Y, Chikayama E, Ohno H, Hino T, Kikuchi J (2009) Evaluation and characterization of bacterial metabolic dynamics with a novel profiling technique, real-time metabolotyping. PLoS One 4:e4893
27. Zhou L, Ding L, Yin P, Lu X, Wang X, Niu J, Gao P, Xu G (2012) Serum metabolic profiling study of hepatocellular carcinoma infected with hepatitis B or hepatitis C virus by using liquid chromatography–mass spectrometry. J Proteome Res 11:5433–5442
28. Ng JC, Wang JP, Zheng B, Zhai C, Maddalena R, Liu F, Moore MR (2005) Urinary porphyrins as biomarkers for arsenic exposure among susceptible populations in Guizhou province, China. Toxicol Appl Pharmacol 206:176–184
29. Maker JR, Struempler A, Chaykin S (1963) A comparative study of trimethylamine-N-oxide biosynthesis. Biochim Biophys Acta 71:58–64
30. Krupp D, Doberstein N, Shi L, Remer T (2012) Hippuric acid in 24-hour urine collections is a potential biomarker for fruit and vegetable consumption in healthy children and adolescents. J Nutr 142:1314–1320
31. Wu J, Shao Y, Liu J, Chen G, Ho PC (2011) The medicinal use of realgar (As_4S_4) and its recent development as an anticancer agent. J Ethnopharmacol 135:595–602
32. Richardson IW, Szerb JC (1974) The release of labelled acetylcholine and choline from cerebral cortical slices stimulated electrically. Br J Pharmacol 52:499–507
33. Ye H-Q, Gan L, Yang X-L, Xu H-B (2006) Membrane-associated cytotoxicity induced by realgar in promyelocytic leukemia HL-60 cells. J Ethnopharmacol 103:366–371
34. Akter KF, Owens G, Davey DE, Naidu R (2005) Arsenic speciation and toxicity in biological systems. Rev Environ Contam Toxicol 184:97–149
35. Beyoğlu D, Idle JR (2012) The glycine deportation system and its pharmacological consequences. Pharmacol Ther 135:151–167
36. Tabatabaie L, Klomp LW, Berger R, de Koning TJ (2010) L-Serine synthesis in the central nervous system: a review on serine deficiency disorders. Mol Genet Metab 99:256–262
37. Chan ECY, Pasikanti KK, Nicholson JK (2011) Global urinary metabolic profiling procedures using gas chromatography–mass spectrometry. Nat Protoc 6:1483–1499